5-2018

Measuring the Double Layer Capacitance of Electrolyte Solutions Using a Graphene Field Effect Transistor

Agatha Ulibarri
Linfield College

Measuring the double layer capacitance of electrolyte solutions using a graphene field effect transistor.

Agatha C. Ulibarri

A thesis submitted in partial fulfillment of the
requirements for the degree of
Bachelor of Science

Department of Physics
Linfield College
McMinnville, OR

May 2018

THESIS COPYRIGHT PERMISSIONS

Please read this document carefully before signing. If you have questions about any of these permissions, please contact the DigitalCommons Coordinator.

Title of the Thesis:

measuring the double layer capacitance of electrolyte solutions using a graphene field effect transistor

Author's Name: (Last name, first name)

Ulibarri, Agatha

Advisor's Name

Crosser, Michael

DigitalCommons@Linfield (DC@L) is our web-based, open access-compliant institutional repository for digital content produced by Linfield faculty, students, staff, and their collaborators. It is a permanent archive. By placing your thesis in DC@L, it will be discoverable via Google Scholar and other search engines. Materials that are located in DC@L are freely accessible to the world; however, your copyright protects against unauthorized use of the content. Although you have certain rights and privileges with your copyright, there are also responsibilities. Please review the following statements and identify that you have read them by signing below. Some departments may choose to protect the work of their students because of continuing research. In these cases, the project is still posted in the repository but content will only be accessible by individuals who are part of the Linfield community.

CHOOSE THE STATEMENT BELOW THAT DEFINES HOW YOU WANT TO SHARE YOUR THESIS. THE FIRST STATEMENT PROVIDES THE MOST ACCESS TO YOUR WORK; THE LAST STATEMENT PROVIDES THE LEAST ACCESS. CHOOSE ONLY ONE STATEMENT.

X I **agree** to make my thesis available to the Linfield College community and to the larger scholarly community upon its deposit in our permanent digital archive, DigitalCommons@Linfield, or its successor technology. My thesis will also be available in print at Nicholson Library and can be shared via interlibrary loan.

OR

_____ I **agree** to make my thesis available **only** to the Linfield College community upon its deposit in our permanent digital archive, DigitalCommons@Linfield, or its successor technology. My thesis will also be available in print at Nicholson Library and can be shared via interlibrary loan.

OR

_____ I **agree** to make my thesis available in print at Nicholson Library, including access for interlibrary loan.

OR

_____ I **agree** to make my thesis available in print at Nicholson Library only.

Updated April 25, 2018

NOTICE OF ORIGINAL WORK AND USE OF COPYRIGHT-PROTECTED MATERIALS:

If your work includes images that are not original works by you, you must include permissions from the original content provider or the images will not be included in the repository. If your work includes videos, music, data sets, or other accompanying material that is not original work by you, the same copyright stipulations apply. If your work includes interviews, you must include a statement that you have the permission from the interviewees to make their interviews public. For information about obtaining permissions and sample forms, see https://copyright.columbia.edu/basics/permissions-and-licensing.html.

NOTICE OF APPROVAL TO USE HUMAN OR ANIMAL SUBJECTS:

If your research includes human subjects, you must include a letter of approval from the Linfield Institutional Review Board (IRB); see https://www.linfield.edu/faculty/irb.html for more information. If your research includes animal subjects, you must include a letter of approval from the Linfield Animal Care & Use Committee.

NOTICE OF SUBMITTED WORK AS POTENTIALLY CONSTITUTING AN EDUCATIONAL RECORD UNDER FERPA:

Under FERPA (20 U.S.C. § 1232g), this work may constitute an educational record. By signing below, you acknowledge this fact and expressly consent to the use of this work according to the terms of this agreement.

BY SIGNING THIS FORM, I ACKNOWLEDGE THAT ALL WORK CONTAINED IN THIS PAPER IS ORIGINAL WORK BY ME OR INCLUDES APPROPRIATE CITATIONS AND/OR PERMISSIONS WHEN CITING OR INCLUDING EXCERPTS OF WORK(S) BY OTHERS.

IF APPLICABLE, I HAVE INCLUDED AN APPROVAL LETTER FROM THE IRB TO USE HUMAN SUBJECTS OR FROM ANIMAL CARE & USE TO USE ANIMAL SUBJECTS.

Signature *Signature redacted* Date 5/16/2018

Printed Name Agatha Ulibarri

Approved by Faculty Advisor *Signature redacted* Date 5/16/2018

Updated April 25, 2018

Thesis Acceptance

Linfield College

Thesis Title: Measuring the double layer capacitance of electrolyte solutions using a graphene field effect transistor.

Submitted by: Agatha C. Ulibarri

Date Submitted: 27th May, 2018

Thesis Advisor: *Signature redacted*

Dr. Michael Crosser

Physics Department: *Signature redacted*

Dr. Jennifer Heath

Physics Department: *Signature redacted*

Dr. Joelle Murray

"If not Arizona, then a land not too far away. Where all parents are strong and wise and capable and all children are happy and beloved. I don't know. Maybe it was Utah."

Raising Arizona

Abstract

When operating graphene field effect transistors (GFETs) in fluid, a double layer capacitance (C_{dl}) is formed at the surface. In the literature, the C_{dl} is estimated using values obtained using metal electrode experiments. Due to the distinctive electronic and surface properties of graphene, there is reason to believe these estimates are inadequate. This work seeks to directly characterize the double layer capacitance of a GFET. A unique method for determining the C_{dl} have been implemented, and data has been obtained for three electrolytes and one ionic fluid. The results yield dramatically lower C_{dl} values than those obtained with metal electrode experiments, and also demonstrate significant asymmetry between electron and hole doped behavior in these ambipolar devices.

Acknowledgements

I would like to acknowledge the help and support of all those who contributed to the success of my undergraduate career. Specifically, I appreciate the Linfield College Collaborative Research Grant for the funding of my research. Many thanks to my thesis committee for helping guide me through the writing process of this document. A special thank you to Alleta Weiss-Maier for challenging me to be a better physics student and for helping support me as a woman in physics. And finally, I extend my gratitude to Dr. Michael S. Crosser; without whom I would not be the person I am today.

Contents

List of Figures

List of Tables

Chapter 1

Introduction

Graphene is a material whose atomic structure is comprised of a single layer of carbon atoms connected in a hexagonal lattice, as illustrated in Figure 1.1. This 2-dimensional sheet of carbon is an exciting and relatively new discovery; having been only theoretically analyzed for decades until the early 2000s[1]. The excitement centered on this recent material discovery involves the unique electronic and structural properties of graphene[2], making the material an interesting and varied subject of study. For instance, carbon is a chemically non-reactive element making it an attractive choice for a variety of sensors; not only does its non-reactivity warrant interest in it as a sensor but also the ability for graphene to change resistance in the presence of small external voltages. This is especially important for biological sensors which would be used in aqueous environments with very small charged molecules in the solution

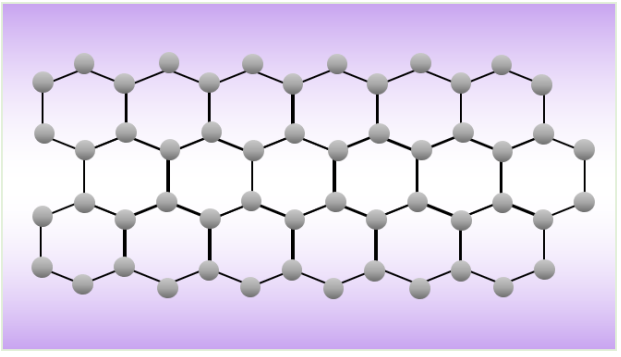

FIGURE 1.1: Schematic of the atomic structure of graphene.

needing to be detected. Graphene is ideal for these small detections due to its higher sensitivity to external electric field than bulk (not 2-dimensional) conducting materials.

Graphene and bulk conductors respond differently to external voltages. For a conducting metal, the presence of an external voltage does not change the charge density of the metal significantly; this response is shown in Figure 1.2. The free electrons that are able to conduct charge through the bulk material remain more or less unaffected when a charge is placed nearby.

The charge affects only approximately the first atomic layer of free electrons which when compared to the immense number of charges in the material have little to no effect on the overall charge density. However, graphene is a single atomic layer so any free charge carriers in the sheet are affected much more than for a bulk conductor; this effect is illustrated in Figure 1.3. This suggests that any charges present in the graphene sheet can be manipulated by an external voltage.

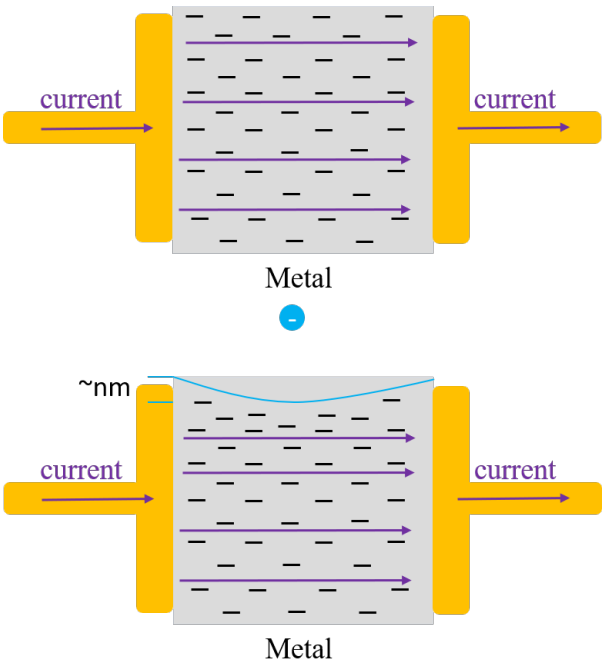

FIGURE 1.2: Illustration of charges passing through a bulk metal conductor with and without the presence of an external electric field. Current is applied to the leads (in gold) and the minimal difference in current flow is highlighted.

Something especially exciting about graphene, is it's ambipolar property; the ability to have either majority electron charge carriers or majority hole charge carriers. This property depends on the applied external electric field. For example, if a large negative voltage is applied then a large amount of holes will be drawn into the graphene sheet and similarly, if a large positive voltage is applied then a large amount

of electrons will be drawn into the graphene sheet. Finally, when no voltage is applied then no charge carriers are present; this point is called the Dirac point, and the resistance of the sheet is highest when the Dirac point is reached.

This suggests that the number of charge carriers in the graphene sheet is proportional to the strength of the external electric field. This makes graphene a very durable and local sensor, enabling it to pick up changes in voltage at very small scales; one study was able to sense the heartbeat of a single heart cell[3]. Due to the small size of graphene sheets they can also be used at a very localized area; targeting and measuring the electrical signal of a single neuron. These initial results already suggest that graphene probes are a promising avenue of research as an alternative to usual metal probes. It also means that understanding and characterizing the electrolyte-graphene interface is critical to furthering the field of 2-dimensional material research.

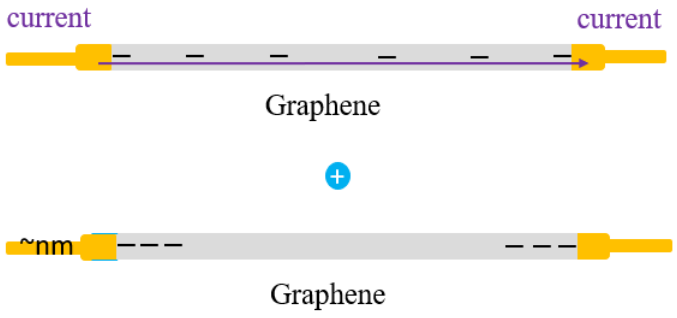

FIGURE 1.3: Illustration of charges passing through a sheet of graphene with and without the presence of an external electric field. Current is applied to the leads (in gold) and the significant difference in current flow is highlighted.

Chapter 2

Experimental Setup

A typical graphene field effect transistor (GFET) chip is pictures in Figure 2.1. Chips of this kind allow for the electronic properties of the graphene to be measured using a variety of equipments and techniques. These GFETs were fabricated using a combination of chemical vapor deposition (CVD) grown graphene transferred to Si wafers, photolithography to shape the graphene, and metal evaporation to deposit metal leads on the GFET chip. The details of device fabrication and electronic measurements are described below.

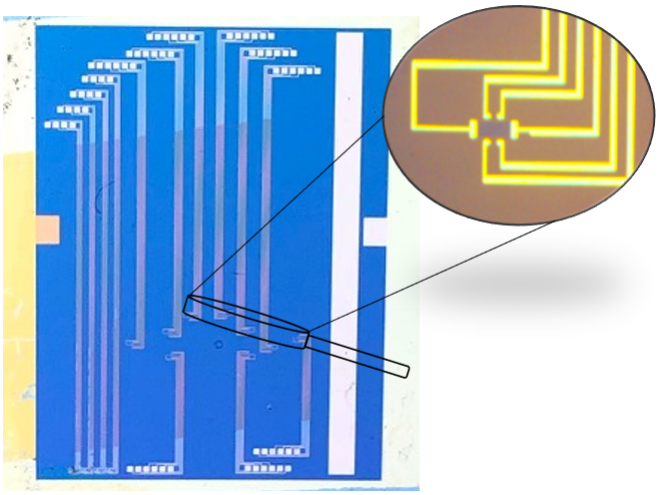

FIGURE 2.1: Picture of a chip with 8 GFETs. One such GFET is shown zoomed in on the upper right-hand corner.

2.1 Device fabrication

CVD grown graphene was procured through ACS material, LLC: https://www.acsmaterial.com/. The graphene is grown on a copper sheet as seen in Figure 2.2[4]. A layer of polymer (PMMA) is spin-coated onto the copper-graphene sheet, the copper is then etched away with a copper etchant purchased from Sigma Aldrich leaving only a sheet of PMMA adhered to mono-layer graphene. This sheet (graphene side down) is then transferred to a Si wafer with a 300nm layer of SiO_2 grown on top. The layer of SiO_2 enables the visual confirmation of mono-layer graphene after transfer. The deep purple color changes more dramatically when a thin layer of material is transferred to its surface then the lighter blue color of Si alone. After the sheet of PMMA-graphene is dried the polymer is removed with an Acetone bath warmed on a hot plate at 60 °C. This bath is allowed to sit for approximately 3 hours before the Si-SiO_2-graphene chip is placed into a room temperature bath of isopropyl alcohol again for approximately 3 hours. From this bath the chip is placed in deionized water nd allowed to soak once this is complete the chip is carefully N_2 dried and ready for the photolithographic step.

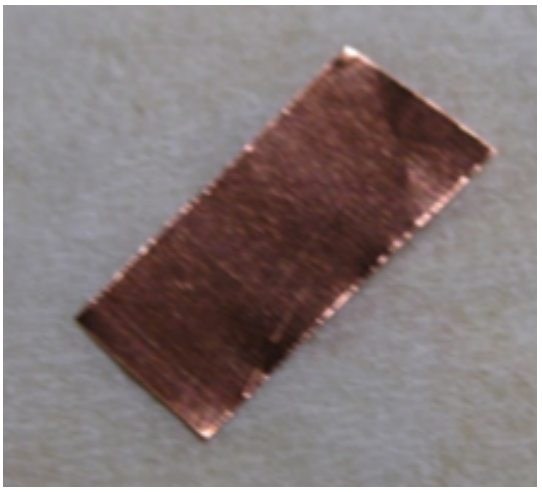

FIGURE 2.2: CVD graphene grown on copper sheeting in preparation for transfer to SiO_2.

The graphene on the Si-SiO_2 is shaped into specific transistor geometries using photolithography. After the Si-SiO_2-graphene chip is dried a photoresist is spin coated on to the surface, see Figure 2.3a. Photoresist is a chemical that becomes soluble in developer when exposed to certain wavelengths of light. For our purposes microposit S1813 was used as our

photoresist which has a sensitivity at 450nm. After the resist is spin coated on and dried at 60 °C for 1 minute, then the chip is exposed to 450nm light in a desired patterned for the graphene;

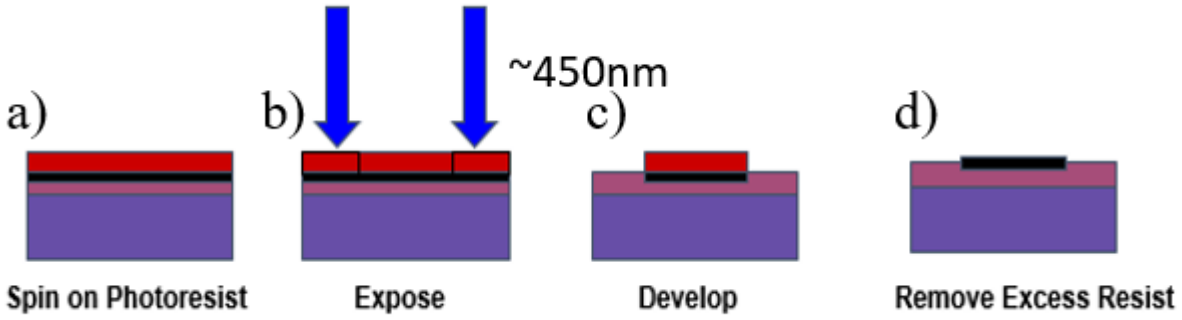

FIGURE 2.3: Photolithography process. Dark purple layer is silicon wafer, the light purple layer is 300nm of SiO_2, the black layer is graphene, and the red layer is photoresist.

shown in Figure 2.3b. The chip is then developed so that the soluble photoresist is removed, after which it is placed in a PE-200 Oxygen Plasma Etcher to remove the unwanted graphene. The result is illustrated in Figure 2.3c. Finally, the excess photoresist is removed in an acetone bath for 1 hour, rinsed with deionized water, and dried with N_2 the final patterned graphene chip is shown in Figure 2.3d. After this process is complete the patterned Si-SiO_2-graphene

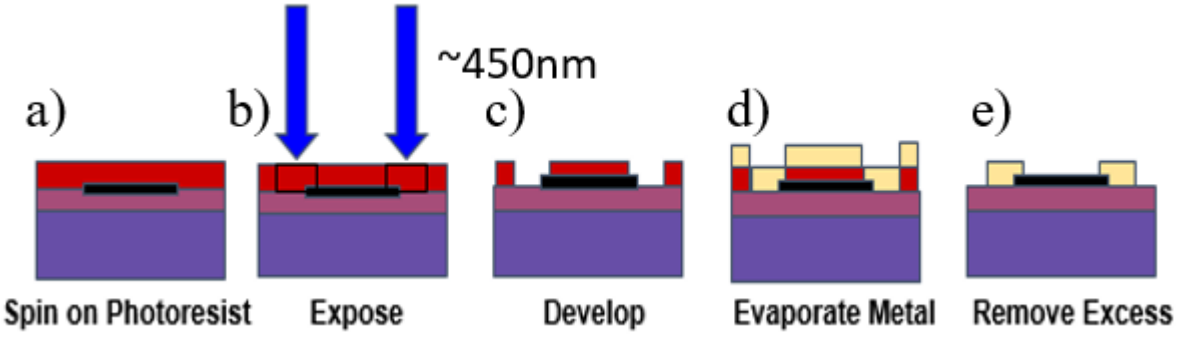

FIGURE 2.4: Photolithography process. Dark purple layer is silicon wafer, the light purple layer is 300nm of SiO_2, the black layer is graphene, the red layer is photoresist, and the yellow layer is gold.

chip is ready for metal leads to be deposited. The process of photolithography and metal evaporation are laid out in more detail in Figure 2.4. The process is quite similar to the graphene patterning recipe discussed previously except that after the lead patterned is exposed and developed, see Figure 2.4c, then approximately 100nm of gold is evaporated onto the chip's surface; see Figure 2.4d. The excess gold and photoresist is removed with a acetone bath on a hot plate at 60 °C, the bath is agitated lightly after about 15 minutes of soak. This continues until all excess metal is removed and then rinsed with deionized water and finally dried with N_2[5].

The preceding process produces a functioning GFET chip and is described from the perspective of the resources available at the Linfield labs. However, the chip used to measure the data quoted in this thesis, Figure 2.1, was fabricated at OSU by the Minot group. Although, the Minot group used similar processes.

2.2 Hall effect measurement

The Hall effect is the production of a voltage, V_{hall}, across a conducting sheet of material with a current flow in the presence of an applied magnetic field that is perpendicular to the current flow. This V_{hall} is due to the Lorentz force acting on the charge carriers of the current; making the charge carriers curve their paths. This causes a difference in charge carrier density from one side of the conducting sheet to the other; hence, a voltage is produced. This effect is illustrated in Figure 2.5. Since graphene is ambipolar, the Hall effect can be measured when holes are the charge carriers present in the graphene, Figure 2.5a, and when electrons are the charge carriers in the graphene, Figure 2.5b. The different charge carriers produce a voltage of opposite sign from each other.

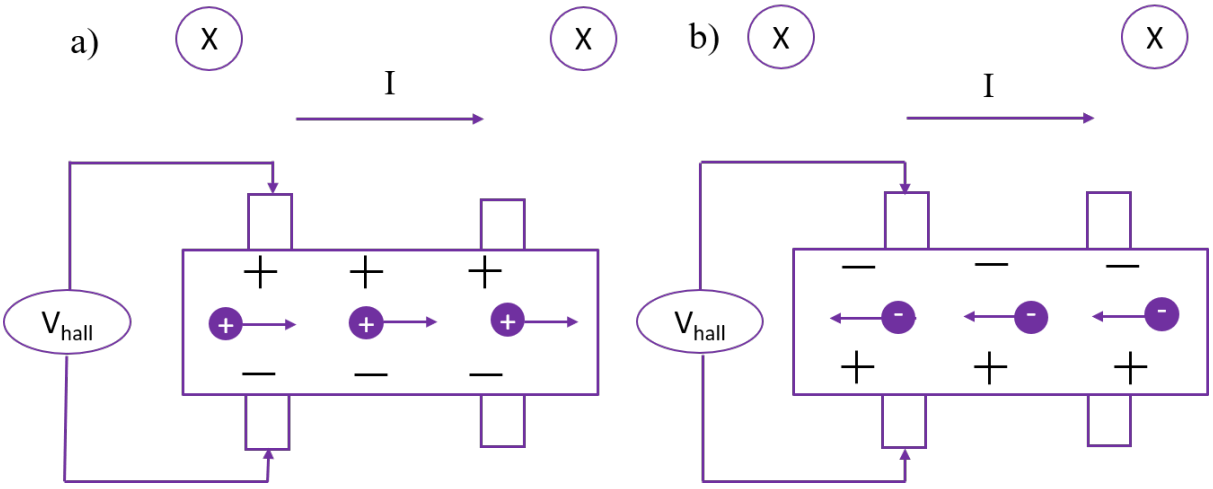

FIGURE 2.5: A magnetic field pointing into the page is shown as well as a current running from left to right. Schematic of a) the Hall effect for hole doped graphene with a positive V_{hall} and b) the Hall effect for electron doped graphene with a negative V_{hall}.

The Hall voltage measurement of our graphene device was made using the following setup. The finished GFET was constructed so that a current could be applied to the sheet of graphene and voltages could be read across the graphene sheet as seen in Figure 2.6a. This geometry is necessary to take V_{hall} measurements from the device. It was also necessary to control the external voltage so that the charge carriers present in the graphene sheet could be tuned from electrons to holes and vice versa. This was done by placing approximately 100μL of electrolyte in a drop on top of the device with a micropipette. Note that three different electrolytes were

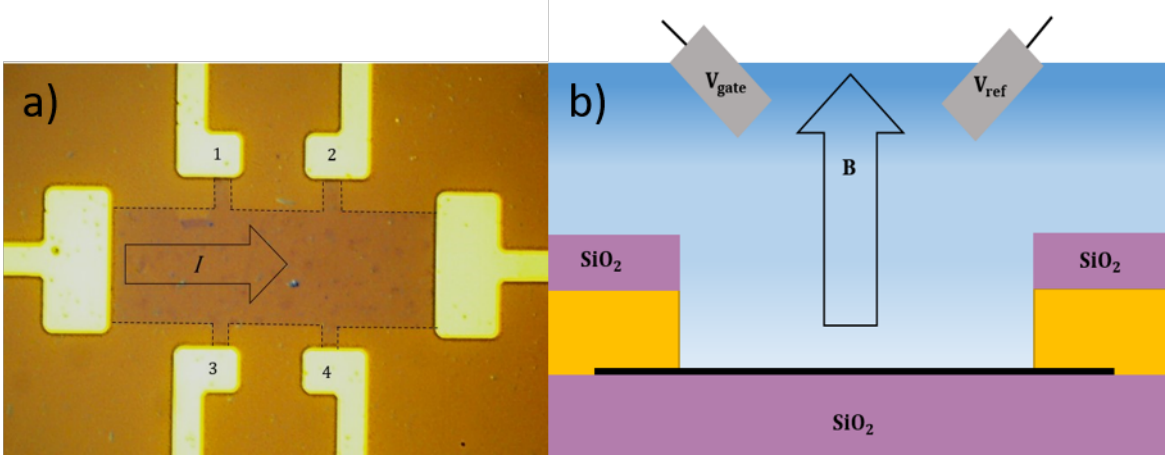

FIGURE 2.6: a) Graphene device with gold leads and direction of current labeled. b) Cross-section of GFET with Pt probes in electrolyte and direction of magnetic field labeled.

tested; 100mM NaCl, 15mM NaCl, 1M Na_2SO_2, and 1-Butyl-3methylimidazolium Hexafluorophosphate. Two platinum probes were inserted into the electrolyte, see Figure 2.6b, and the GFET was inserted into an electro-magnet; maintaining a magnetic field of approximately ±500mT. A Kiethly 2000 sourcemeter applied a constant current of 5μA. The gate probe applied the external voltage required to tune the type and number of charge carriers in the graphene sheet. This voltage, V_{gate}, was controlled by the DC voltage output on the SR830 Lock In Amplifier and swept from 0V to approximately 0.8V at a rate of 100 samples per second. A circuit diagram of the experiment is illustrated in Figure 2.7. The second probe

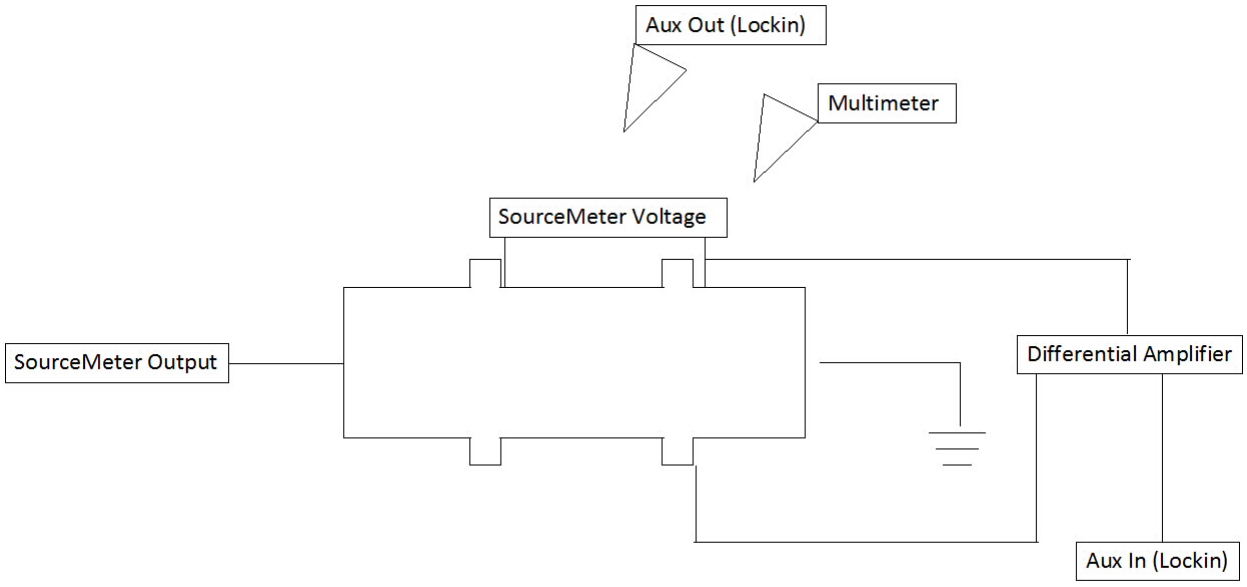

FIGURE 2.7: Circuit diagram of the measurement setup.

in the electrolyte, the reference probe, actually measures the voltage that the graphene effectively sees, the V_{ref}. The reason for this is because the electro-chemistry of the probe-electrolyte interface makes direct values applied to the gate probe unreliable. The reference probe importance is highlighted in Figure 2.9, where hysteresis is apparent in the V_{gate} curve but the V_{ref} curve seemingly removes this hysteresis. An example of the Hall measurement is shown in Figure 2.8.The peak of highest V_{xx} corresponds to the highest resistance and the state in which no charge

carriers are available in the graphene sheet. This is the Dirac point and corresponds to the point at which graphene switches from holes to electrons in Figure 2.8b, illustrated by the flip in sign of the V_{hall} measurement.

A third voltage measurement was made for the GFET; the effective resistance of the graphene sheet,V_{xx}. These measurements were made with the Kiethly 2000 sourcemeter and correspond to taking the voltage between leads 1 and 2 in Figure 2.6a. The program, LabVIEW was used to collect the voltage measurements; V_{xx}, V_{gate}, and V_{ref}.

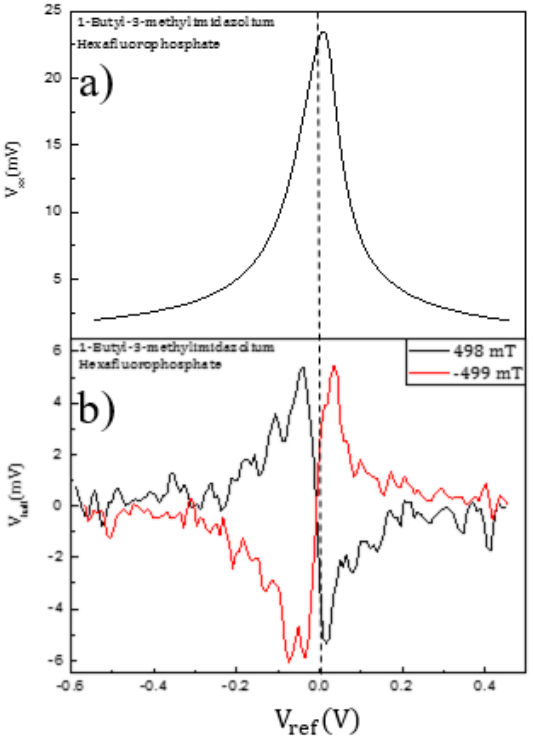

FIGURE 2.8: Data showing a) V_{xx} and b) V_{xx} as a function of V_{ref}

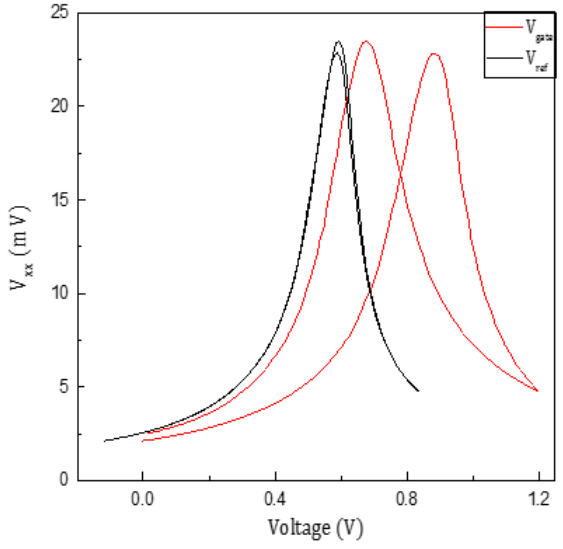

FIGURE 2.9: V_{xx} versus V_{gate} (red) and V_{ref} (black) plot.

Chapter 3

Theory

Consider a metal electrode within an electrolyte as seen in Figure 3.1. When a potential is applied to the electrode, ions in the electrolyte will be attracted to the electrode surface; creating an electrostatically charged layer in the electrolyte with a thickness, $\lambda = d + x$[6]. The density of charges is highest at the electrode-electrolyte interface and then remains dense for some depth away from the electrode until it drops off to equilibrium in the bulk electrolyte, see Figure 3.2. This causes a separation of charge with two distinct thicknesses; one with a thickness of x, called the Stern layer, which corresponds directly to the size of the ions being attracted most acutely to the charged electrode, and another

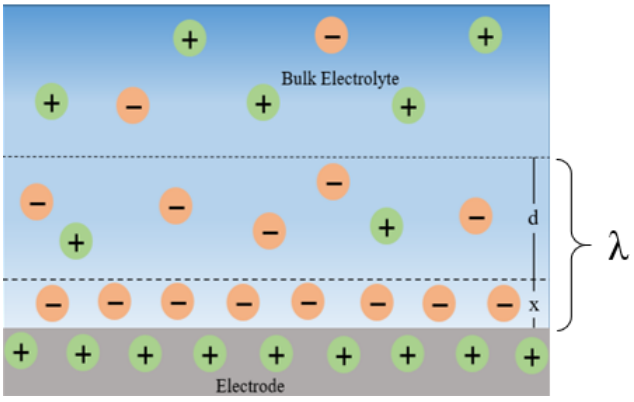

FIGURE 3.1: Illustration of surface interactions of a charged metal electrode in an electrolyte solution. The layer of charges labeled with a thickness x form the Stern layer, the layer labeled with a thickness d form the diffuse layer, and $\lambda = x + d$.

with a thickness of d, called the diffuse layer, which is composed of charges that are being pulled from the bulk electrolyte to screen out the potential applied to the electrode.

The two separations of charge form two capacitors in series. The total capacitance of this system is called the double layer capacitance, C_{dl}. Each capacitor in this system, C_x and C_d, can be modelled as parrallel plate capacitors with the form, $C = \frac{k\varepsilon_0 A}{l}$ where l is the distance between the plates, k is the permittivity of the dielectric in our case water, A is the area of the plates, and ε_0 is the permittivity of free space. Then,

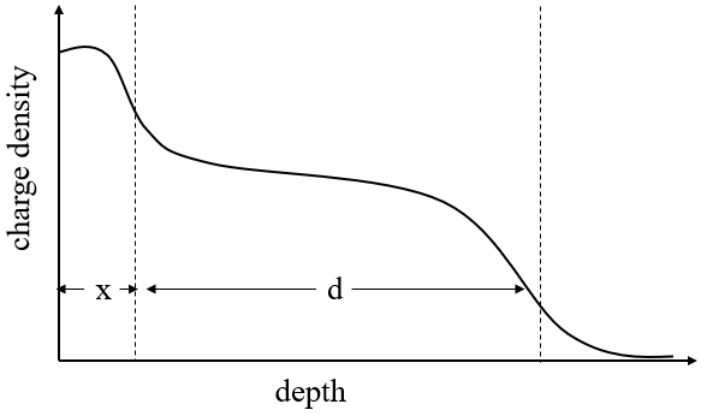

FIGURE 3.2: Diagram of relative charge density as a function of distance from the electrode. The Stern distance is labeled x and the diffuse distance is labeled d.

$$\begin{aligned}
\frac{1}{C_{dl}} &= \frac{1}{C_d} + \frac{1}{C_x} \\
C_{dl} &= \frac{C_x C_d}{C_{tx} + C_d} \\
&= \frac{\frac{(k\varepsilon_0 A)^2}{dx}}{\frac{k\varepsilon_0 A}{x} + \frac{k\varepsilon_0 A}{d}} \\
&= \frac{k\varepsilon_0 A}{d+x} \\
&= \frac{k\varepsilon_0 A}{\lambda}. \qquad (3.1)
\end{aligned}$$

So it is possible to predict theoretically the C_{dl} for a known x and d value where x is the effective diameter of the ion, and d can be found with the Debye-Hückle approximation with $d \propto \frac{1}{\sqrt{c}}$ where c is the concentration of the electrolyte[6].

However, this model depends on a bulk metal electrode and does not take into consideration the unique electronic properties of graphene. The literature generally quotes these metal electrode experiments for the C_{dl} values of graphene devices but if these values were unreliable then quotes for graphene properties such as mobility may also be affected. Mobility is the measure of how easily charge carriers are able to move through a material and it is often determined for graphene using the following relationship;

$$\mu = \frac{1}{C}\frac{\Delta\sigma}{\Delta V_{gate}} \tag{3.2}$$

where C is the total capacitance of the GFET system and σ is the conductivity of the graphene[7].

The total capacitance, C, of the GFET can be determined by analyzing the capacitances and voltages of the system as seen in Figure 3.3. The quantum capacitance, C_Q, arises from graphene's low density of states, and is defined as;

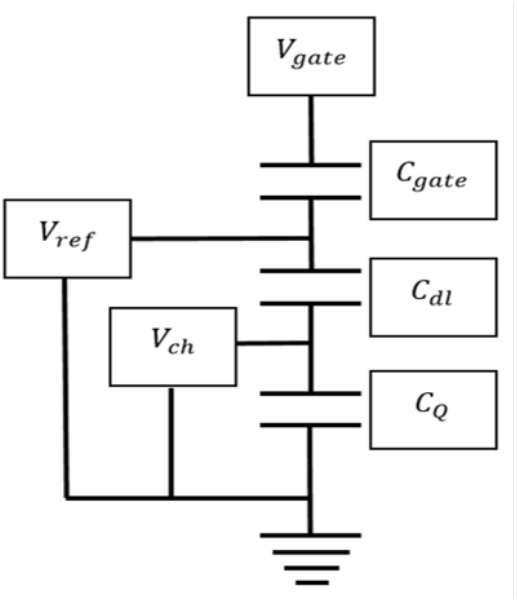

FIGURE 3.3: A schematic of the voltages formed in the system of Figure 2.6b.

$$C_Q = \frac{e^2}{\hbar v_F \sqrt{\pi}}\sqrt{n} \tag{3.3}$$

where e is simply the elemental charge, $\hbar$ is the reduced Planck constant, v_F is the Fermi velocity given by approximately 10^6 ms^{-1}, and n is the number of charge carriers in the graphene sheet[8]. Then the total capacitance is just the quantum capacitance and double layer capacitance in series and is defined by;

$$C = \frac{C_{dl}C_Q}{C_{dl} + C_Q}. \tag{3.4}$$

Capacitance is defined by; $Q = \Delta VC$, where $Q = en$ is the total charge and ΔV is the change in voltage across the capacitor. Using this definition we can write V_{ref} as simply the sum of the voltages across each capacitor, and those voltages are given by;

$$V_Q = \frac{en}{C_Q} \tag{3.5}$$

$$V_{dl} = \frac{en}{C_{dl}}. \tag{3.6}$$

Now,

$$\begin{aligned} V_{ref} &= V_Q + V_{dl} \\ &= \frac{en}{C_Q} + \frac{en}{C_{dl}} \end{aligned}$$

substitute in equation 3.3

$$\begin{aligned} &= \frac{en}{\frac{e^2\sqrt{n}}{\hbar v_F \sqrt{\pi}}} + \frac{en}{C_{dl}} \\ &= \frac{\hbar v_F \sqrt{\pi n}}{e} + \frac{en}{C_{dl}}. \end{aligned} \tag{3.7}$$

we have V_{ref} as a function on n and C_{dl}[9]. From this C_{dl} can be extracted as long as n is known. We can measure n using the Hall measurement discussed in Chapter 2. The Hall voltage is defined by;

$$V_{hall} = \frac{IB}{en} \tag{3.8}$$

where I is the current applied and B is the strength of the magnetic field applied[7]. From this it is found that $n \propto \frac{1}{V_{hall}}$.

With the information provided from equations 3.7 and 3.8 it is possible to determine the C_{dl} for a GFET device without relying on the usual metal probe measurement values. This theoretical background was implemented to infer a value of C_{dl} for a GFET system.

Chapter 4

Results and Analysis

Measurements of V_{hall} and V_{ref} were collected for a GFET in different fluid environments. These measured values were used to determine a C_{dl} value for the following solutions; 100mM NaCl, 15mM NaCl, 1M Na2SO2, and 1-Butyl-3methylimidazolium Hexafluorophosphate. The analysis process for the collected data and the results for each measured fluid are presented in this chapter. In addition a summary of the results and a discussion of their implications, are examined.

4.1 Analysis setup

The theory developed in chapter 3 allowed a method for fitting raw data of V_{hall} as a function of V_{ref} to extrapolate C_{dl} to be determined. An intrinsic charge carrier parameter n^* is considered as well in these fits so that equation 3.7 becomes;

$$V_{\text{ref}} = \frac{\hbar v_F \sqrt{\pi n}}{e} + \frac{en}{C_{\text{dl}}} + n^*. \tag{4.1}$$

The intrinsic number of charge carriers is attributed to charged impurities in the graphene sheet[8].

A user-defined Origin 2016 nonlinear curve fit function was created to fit equation 3.8, an example of this fit function can be seen in Appendix A. Note that n itself was not fit directly but rather n^{-1}, this is because the V_{hall} measurements taken were noisy and at some points approached or crossed 0V. If n were to be fit directly then we would be dividing by zero and the values of C_{dl} and n^* would be unreliable. An example of a V_{hall} versus V_{ref} graph exhibiting the aforementioned noise and nonlinear curves of best fit are shown in Figure 4.1. It is also apparent in Figure 4.1 that the C_{dl} values for when the graphene sheet has majority holes, the blue fit, is different than that for when the graphene sheet has majority electrons, the red fit.

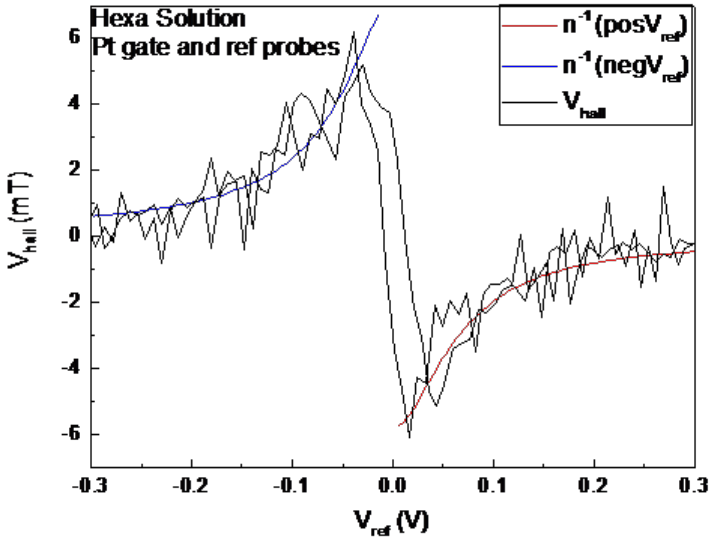

FIGURE 4.1: V_{hall} versus normalized V_{ref} for 1-Butyl-3methylimidazolium Hexafluorophosphate. Theoretical lines for majority hole and electron charge densities shown separately as blue and red respectively

Note that the Dirac point did not occur at $V_{ref} = 0V$ so the reference voltage was normalized by subtracting this Dirac voltage, V_D, amount. Similarly the n^* values were subtracted from raw n measurements to normalize the results, this essentially just shifted the graph down to zero to match the theoretical plots. These fits were found for each tested solution and plots of $n - n^*$ versus $V_{ref} - V_D$ were made with theoretical lines for the corresponding C_{dl} fits. An

example of one of these plots is shown in Figure 4.2. The electron side fit is shown in red for 100mM NaCl. The remaining plots can be seen in Appendix B. It must be noted that as C_{dl} increases to infinity equation 3.7

becomes;

$$V_{\text{ref}} = \frac{\hbar v_F \sqrt{\pi n}}{e} \qquad (4.2)$$

This means there is an intrinsic limit to any n versus V_{ref} plot. This limit, known as the quantum limit, is shown in Figure 4.2 as the dashed line.

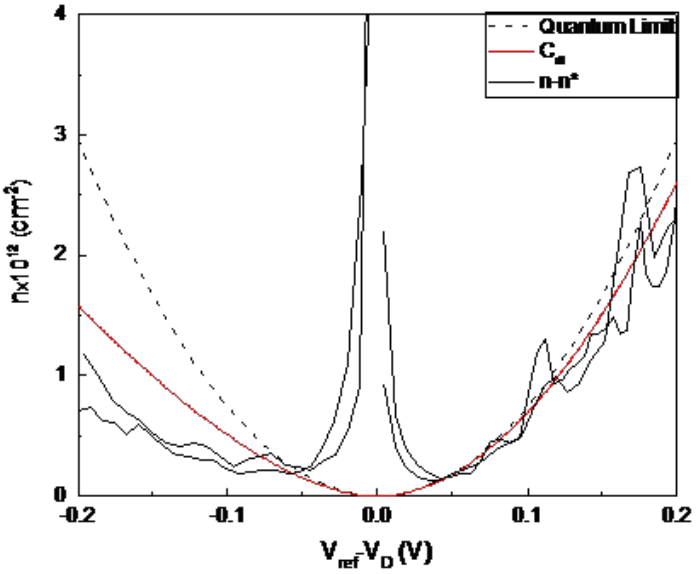

FIGURE 4.2: 100mM NaCl. n versus normalized V_{ref} for raw data (black), the fits of C_{dl} (purple), and the quantum limit (dashed.)

4.2 Discussion

Table 1 outlines the measured C_{dl}

of every tested solution and compares that value to the metal electrode theory predicted values. The uncertainty given in Table 1 were given by origins user defined function fitting software.

TABLE 4.1: Predicted and measured values of C_{dl} for NaCl, Na_2SO_4, and 1-Butyl-3methylimidazolium Hexafluorophosphate. This illustrates the asymmetry in data collected. Note that all measured values are 50% or lower than the predicted values.

Solution	Predicted C_{dl} (μFcm^{-2}): holes	Predicted C_{dl} (μFcm^{-2}): electrons	Measured C_{dl} (μFcm^{-2}): holes	Measured C_{dl} (μFcm^{-2}): electrons
Hexafluorophasphate	NA	20.0	3.1 $\pm$ 0.4	5.3 $\pm$ 0.9
NaCl (15mM)	11.4	14.5	2.5 $\pm$ 0.2	7.0 $\pm$ 1.0
NaCl (100mM)	15.2	21.2	2.3 $\pm$ 0.2	17 $\pm$ 4.0
Na_2SO_4 (1M)	13.0	14.4	2.2 $\pm$ 0.4	5.2 $\pm$ 1.0

They represent the standard deviation in the calculated parameters and it is worth noting that the uncertainty is of the same order of magnitude for each value of C_{dl}, except for electron measurement of the 100mM NaCl, implying that the fits were consistent. Another indication of our data being consistent with the theory is the fact that our plot of n versus V_{ref} lies below the quantum limit curve, see Figure 4.2. A last indication of consistency with theory is that the values found from the fitting parameter, n^* ranged from 2.2-4.7$\times 10^{11}$cm^{-2}. Since each n^* had the same order of magnitude this implies that our fits were of good approximation because n^* is an intrinsic property of the graphene sheet and should not change with fluid variation.

Finally, it was found that each fluid exhibited asymmetry in C_{dl} values not expected form the theory. The hole doped graphene measurements yielded C_{dl} values of approximately the same magnitude and were significantly lower than the measured electron doped values. The slopes of the n versus ΔV plot in Figure 4.3 are proportional to capacitance since $C = ne/\Delta V$. The significant differences in slope highlights the asymmetry of the C_{dl} data.

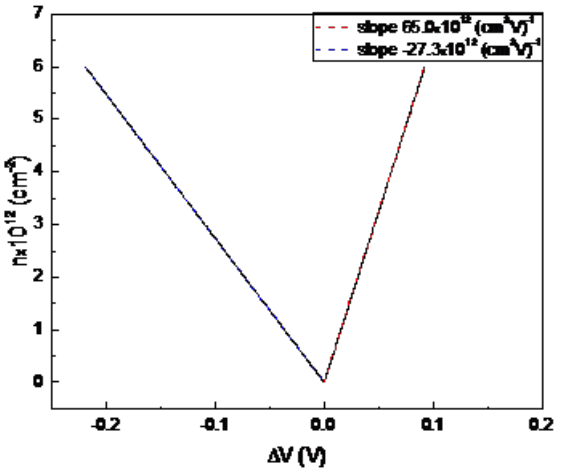

FIGURE 4.3: Difference of voltage at the quantum limit (equation 3) and with the determined C_{dl} (equation 2). The asymmetry found is evident in the difference of slopes given for majority hole charge densities (blue) and majority electron densities (red). Data taken with 1M Na_2SO_4.

Chapter 5

Conclusions

It was the subject of this thesis to investigate the double layer capacitance of a graphene-electrolyte system. This was accomplished and useful data were taken to fully understand the liquid gated GFETs electronic properties. It is necessary to understand and characterize the C_{dl} completely in order to maintain a good understanding of the GFET-electrolyte system.

A unique method for determining the C_{dl} was implemented. The number of charge carriers in the graphene was measured as a function of the V_{fluid} and a fitting function was used to extract the C_{dl} value within a statistically reasonable uncertainty. It was found that our data exhibit asymmetry depending on the type of charge carrier present in the graphene. This suggests a difference of C_{dl} when holes are present in the graphene than when electrons are present. This effect has been discovered in the literature but no satisfactory reason has been determined. It may have to do with the size of ions affecting the distance of the Stern layer or it may have to do with charge traps in the graphene sheet itself. Finally, our data suggest that C_{dl} is lower above graphene than for a metal electrode. This is a finding that has consequences across the field of graphene research. For instance, measurements of mobility and the known sensitivities

of biological GFET sensors would be affected by our results.

Investigation of the double layer capacitance for a GFET can be expanded further. In this thesis, data were collected for three electrolytic solutions. However, data for a larger range of electrolytes and concentrations would improve the knowledge of how the C_{dl} differs from previously quoted values and elucidate a yet unknown relationship between C_{dl} above graphene and metal. Further, a more comprehensive examination of liquids with different sized ions will help to rule out the cause of asymmetry in our data. If we do not continue to see the asymmetry when the ion sizes are controlled, then we will be able to investigate other properties that could contribute to the asymmetry such as trapped charges in the graphene sheet.

Appendix A

Fitting Function

Nonlinear Curve Fit (ChargeDensity (User)) (2/26/2018 22:39:46)

Notes

Description	Nonlinear Curve Fit
User Name	mcrosse
Operation Time	2/26/2018 22:39:46
Iteration Algorithm	Levenberg Marquardt
Model	ChargeDensity (User)
Number of Parameters	2
Number of Derived Parameters	0
Number of Datasets	1
Equation	n=nstar+beta^2*((-Cdl+ sqrt(Cdl^2+4*gamma*Cdl*abs(Vref))/2/gamma)^2
Report Status	New Analysis Report
Special Input Handling	
Data Filter	No

Input Data

		Dep/Indep	Data	Range	Weight Type
nneg	Vref	Indep	[Book22]Sheet1!C"Vneg"	[1*:41*]	No Weighting
	n	Dep	[Book22]Sheet1!D"nneg"	[1*:41*]	No Weighting

Parameters

		Value	Standard Error	t-Value	Prob>|t|	Dependency
nneg	Cdl	0.02115	0.00302	7.00834	2.08732E-8	0.69254
	nstar	5.53792E15	3.52406E14	15.7146	0	0.69254

Reduced Chi-sqr = 1.56550472105E30
COD(R^2) = 0.70476993814354
Iterations Performed = 5
Total Iterations in Session = 5
Fit converged. Chi-Sqr tolerance value of 1E-9 was reached.
Standard Error was scaled with square root of reduced Chi-Sqr.
Constants : beta=860000000 gamma=0.239

Statistics

Summary

	Cdl		nstar		Statistics	
	Value	Standard Error	Value	Standard Error	Reduced Chi-Sqr	Adj. R-Square
nneg	0.02115	0.00302	5.53792E15	3.52406E14	1.5655E30	0.6972

ANOVA

		DF	Sum of Squares	Mean Square	F Value	Prob>F
nneg	Regression	2	3.3544E33	1.6772E33	1071.3477	0
	Residual	39	6.10547E31	1.5655E30		
	Uncorrected Total	41	3.41545E33			
	Corrected Total	40	2.06804E32			

Fitted Curves Plot

nneg

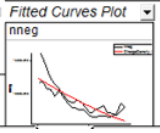

FIGURE A.1: Nonlinear curve fit details showing equation used, fitting parameters, and independent-dependent variables.

Appendix B

Other Fluid Graphs

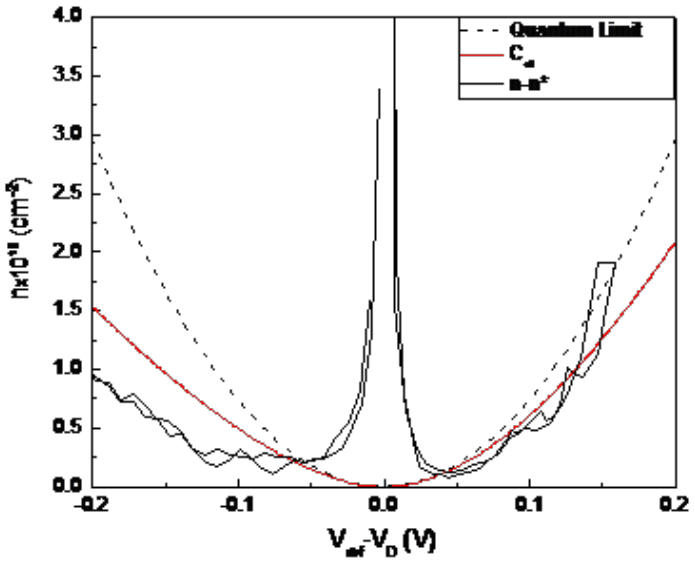

FIGURE B.1: 1M Na_2SO_4. n versus normalized V_{ref} for raw data (black), the fits of C_{dl} (purple), and the quantum limit (dashed.)

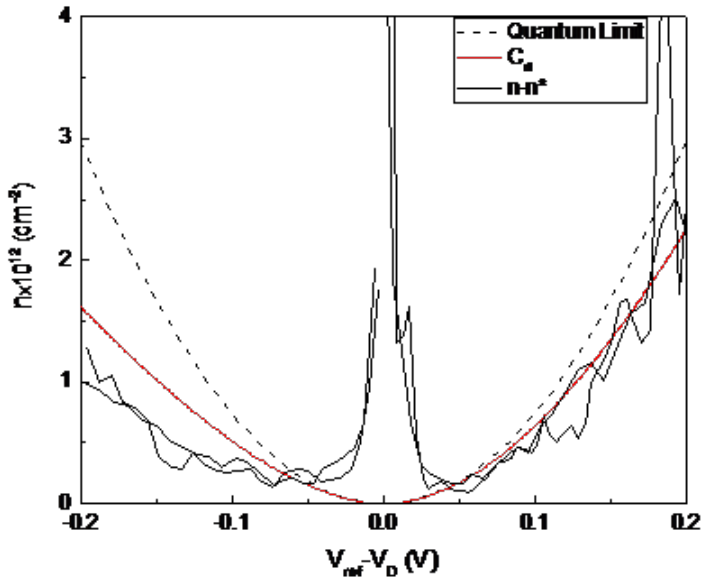

FIGURE B.2: 15mM NaCl. n versus normalized V_{ref} for raw data (black), the fits of C_{dl} (purple), and the quantum limit (dashed.)

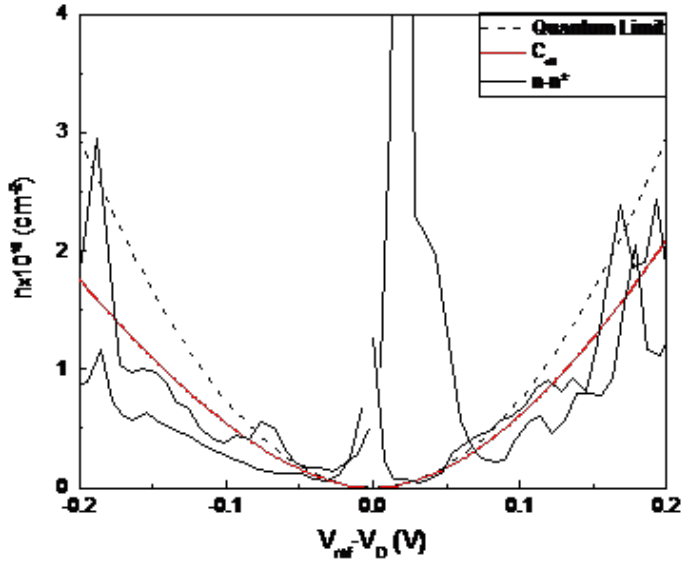

FIGURE B.3: 1-Butyl-3methylimidazolium Hexafluorophosphate. n versus normalized V_{ref} for raw data (black), the fits of C_{dl} (purple), and the quantum limit (dashed.)

Bibliography

[1] Novoselov, K.S. et al. Electric field effect in atomically think carbon films. *Science*, 306: 666–669, 2004.

[2] Ishigami, M., Chen, J.H., Cullen, W.G., Fuhrer, M.S., and Williams, E.D. Atomic structure of graphene on SiO_2. *Nano Letters*, 7(6):1643–1648, 2007.

[3] Cheng, Z. et al. Sensitivity limits and scaling of bioelectronic graphene transducers. *Nano Letters*, 13:2902–2907, 2013.

[4] Mattevi, C., Kim, H., and Chhowalla, M. A review of chemical vapour deposition of graphene on copper. *Journal of Materials Chemistry*, 2010.

[5] M.B. et al Lerner. Scalable production of highly sensitive nanosensors based on graphene functionalized with a designed g protein-coupled receptor. *Nano Letters*, 14:2709–2714, 2014.

[6] Ghosh, P. Electrostatic double layer force: Part II. *NPTEL Chemical Engineering*, Tutorial. URL http://nptel.ac.in/courses/103103033/module3/lecture3.pdf.

[7] Crosser, M.S., Brown, M.A., McEuen, P.L., and Minot, E.D. Determination of the thermal noise limit of graphene biotransistors. *Nano Letters*, 2015.

[8] Xia, J. et al. Measurement of the quantum capacitance of graphene. *Nature Nanotechnology*, 4:505–509, August 2009.

[9] Brown, M. Graphene biotransistors, an exploration of neurosensing and biofilm -sensing applications. *Dissertation*. URL http://minotlab.physics.oregonstate.edu/sites/minotlab.physics.oregonstate.edu/files/pdfs/MorganBrownA2017.pdf.